

# *Tropical moist convection an important driver of Atlantic Hadley circulation variability*

Article

Published Version

Creative Commons: Attribution 4.0 (CC-BY)

Open Access

Tomassini, L. and Yang, G.-Y. ORCID: <https://orcid.org/0000-0001-7450-3477> (2022) Tropical moist convection an important driver of Atlantic Hadley circulation variability. Quarterly Journal of the Royal Meteorological Society, 148 (748). pp. 3287-3302. ISSN 1477-870X doi: 10.1002/qj.4359 Available at <https://centaur.reading.ac.uk/108601/>

It is advisable to refer to the publisher's version if you intend to cite from the work. See [Guidance on citing](#).

To link to this article DOI: <http://dx.doi.org/10.1002/qj.4359>

Publisher: Royal Meteorological Society

All outputs in CentAUR are protected by Intellectual Property Rights law, including copyright law. Copyright and IPR is retained by the creators or other copyright holders. Terms and conditions for use of this material are defined in the [End User Agreement](#).

[www.reading.ac.uk/centaur](http://www.reading.ac.uk/centaur)

**CentAUR**

Central Archive at the University of Reading

Reading's research outputs online



## RESEARCH ARTICLE

# Tropical moist convection as an important driver of Atlantic Hadley circulation variability

Lorenzo Tomassini<sup>1</sup>  | Gui-Ying Yang<sup>2</sup> <sup>1</sup>Met Office, Exeter, UK<sup>2</sup>Climate Directorate, National Centre for Atmospheric Science, Department of Meteorology, University of Reading, Reading, UK**Correspondence**

L. Tomassini, Met Office, FitzRoy Road, Exeter EX1 3PB, UK.

Email:

[lorenzo.tomassini@metoffice.gov.uk](mailto:lorenzo.tomassini@metoffice.gov.uk)**Funding information**

Natural Environment Research Council, Grant/Award Number: NE/R000034/1

**Abstract**

The exact role of moist deep convection and associated latent heating in the tropical Hadley circulation has been debated for many years. This study investigates the connection between moist convection and the strength of the upper-level meridional circulation over the tropical Atlantic, focusing mainly on one particular boreal winter season. There is a close relationship between events of strong organised deep convection and enhanced meridional upper-level wind on many occasions. A process-based analysis of specific events suggests that moist convection impacts Hadley circulation variability on time-scales of days to months through equatorial wave dynamics. Equatorial waves play an important role, both directly by contributing to the Hadley circulation via their meridional wind component and also indirectly by triggering moist convection through low-level convergence. Specific Hadley circulation surge events, short-term, regionally confined intensifications of the upper-level meridional circulation, can be attributed to enhanced organised moist convection and equatorial wave activity in many cases, with implications for trade wind cloudiness. The findings thus elucidate how the mean Hadley circulation is shaped by and composed of temporally and spatially varying convection–circulation interactions.

**KEYWORDS**

convection–circulation coupling, equatorial waves, Hadley circulation, tropical convection

## 1 | INTRODUCTION

From a time-mean and zonal-mean perspective, the Hadley circulation is driven by meridional temperature gradients, and ultimately by latitudinal variations in solar insolation. In this view, tropical moist convection can be considered to be in near-equilibrium with its environment and to act to reduce the potential energy,

created by large-scale processes, available to generate kinetic energy of *large-scale motion* (Emanuel *et al.*, 1994). As a consequence of this convective adjustment process, the large-scale ascent of the Hadley circulation is responding to an effective, positive static stability. In this equilibrium picture, moist convection therefore dampens the Hadley circulation overall, and its main role is to establish a one-to-one relationship between the subcloud layer

This is an open access article under the terms of the Creative Commons Attribution License, which permits use, distribution and reproduction in any medium, provided the original work is properly cited.

© 2022 Crown copyright and The Author. *Quarterly Journal of the Royal Meteorological Society* published by John Wiley & Sons Ltd on behalf of the Royal Meteorological Society. This article is published with the permission of the Controller of HMSO and the Queen's Printer for Scotland.

entropy and the virtual temperature of the atmosphere (Brown and Bretherton, 1997; Emanuel, 1998; Neelin and Zeng, 2000; Yano and Plant, 2012).

Locally and on shorter time-scales, however, nonequilibrium convection can be a source of energy for large-scale motions such as the Hadley circulation, as pointed out by Stevens *et al.* (1997). The correlation between latent heating from convection and temperature anomalies in the atmosphere created by large-scale processes is not always negative. Convection does not just consume available potential energy, it can cooperate positively with large-scale motion. An important argument in this context is that convection in the tropical atmosphere is not just a small-scale phenomenon (Mapes, 1997), and the separation between large-scale and convective processes is ambiguous (Pan and Randall, 1998). Individual convective clouds are small and short-lived compared with the horizontal dimensions and time-scales of circulations like the Hadley Cell. However, organised convective systems in the Tropics can have impacts on circulations over large distances, because latent heating from convection in the upper tropical troposphere may create large-scale waves such as, for instance, those described by the highly successful theory of equatorial waves (Matsuno, 1966; Gill, 1980; Mapes, 2000).

Hoskins *et al.* (2020) and Hoskins and Yang (2021) recently presented a comprehensive and detailed investigation of the Hadley circulation, arguably the most fundamental feature of tropical weather and climate. They suggested complementing and refining the traditional zonal-mean and time-mean theory in two ways: the two studies acknowledge the central role of moist convection as a driving factor of Hadley circulation variability, and suggest that the asymmetries in longitude and fluctuations on time-scales of days to months are of order one importance in the upper branch of the Hadley Cell. The two aspects are connected: the temporal and zonal variations of the Hadley circulation are a necessary, although in itself not sufficient, precondition for localised organised convection to play an active role in governing Hadley circulation variability, and not just act as a passive counterweight (Tomassini, 2020).

The key observation is that, where and when there is active deep convection, the Coriolis parameter is approximately balanced by relative vorticity due to strong, regionally confined outflow of air into the winter hemisphere (Hoskins *et al.*, 2020). In other words, organised moist convection is the main influencing factor of upper-level vorticity modulating the strength of the local Hadley circulation on time-scales of days to months. This is an extension of the more traditional view, which emphasizes the zonal-mean balance between relative vorticity flux and

the Coriolis force, and the zonal-mean solar heating and subsequent meridional temperature gradient as principal control.

In the present study it is shown, based on the detailed analysis of a boreal winter season over the tropical Atlantic, that it is the regions and times of active convection that predominantly lead to upper-tropospheric outflow and structures that average to result in the mean flow toward the opposite pole, and the steady and transient fluxes of momentum and vorticity that balance the Coriolis terms. Thus, longitudinal and temporal fluctuations of tropical moist convection are key factors in governing regional Hadley Cell strength and variability.

It is well established that equatorial waves are not only a product of latent heat release by moist convection, but also modulate tropical convection (Kiladis *et al.*, 2009; Ferrett *et al.*, 2020; Ayesiga *et al.*, 2021). Therefore the two-way interaction between equatorial atmospheric waves and moist convection impacts the strength of the meridional flow in the Tropics in two ways. The circulation characteristics of the wave can have a meridional component and thus contribute directly to variability in the meridional wind (Yang *et al.*, 2003; Yang *et al.*, 2007a; Yang *et al.*, 2007b; Yang *et al.*, 2007c). Alternatively, the wave can affect the meridional circulation indirectly by triggering or enhancing moist convection, which, in turn, produces upper-level outflow and meridional motion.

Similar conclusions were reached by Schwendike *et al.* (2021), who investigated the effect of enhanced and suppressed MJO-related convection on the strength and poleward extent of the local Hadley circulations. In many ways, the idea that moist convection is an important factor in the driving processes of the Hadley circulation is at the heart of the “hot towers hypothesis” formulated by Riehl and Malkus (1958) (see also Fierro *et al.* (2009)). Moreover, previous work highlighted the importance of zonal asymmetries and physical processes related to the presence of continents for Hadley Cells, aspects that are not captured by axisymmetric models (Cook, 2003; Cook, 2004). In the present study, we focus on one particular boreal winter season over the tropical Atlantic in order to be able to understand better the detailed structure and variability of the regional Hadley circulation and the governing processes behind it. A related motivation for investigating the period in more detail was the Elucidating the Role of Clouds–Circulation Coupling in Climate (EUREC<sup>4</sup>A) observational field campaign (Stevens *et al.*, 2021), which took place in January and February 2020. Large-scale conditions had a strong influence on cloudiness and cloud patterns over subtropical subsidence regions during the observation period, a topic that is touched upon in Section 4.

## 2 | RELATIONSHIP BETWEEN HADLEY CIRCULATION AND TROPICAL CONVECTION VARIABILITY

In the present work we mainly restrict our attention to the tropical Atlantic and the season December 2019–February 2020. The rationale is that a detailed analysis of one single season allows for unearthing of some basic principles and characteristics of Hadley circulation variability and, at the same time, better understanding of the processes behind it. Nevertheless, it is instructive first to consider a few basic climatological aspects, as revealed by the ERA5 reanalysis (Hersbach *et al.*, 2020) data (Figure 1).

The wind climatology at 200 hPa shows a distinct anti-cyclonic circulation over the western part of the South American continent and a cyclonic circulation over the western tropical Atlantic ocean. In between, over the eastern part of the South American continent, the strongest meridional wind is observed. The main upper-level northward flow deflects to the right to form the subtropical jet north of the Equator.

Over the tropical Atlantic, the midtropospheric vertical motion that can be attributed to the Walker circulation is small, and the meridional Hadley circulation dominates (Schwendike *et al.*, 2015). Thus, the vertical pressure velocity at 500 hPa is a good measure for the position and strength of the local Hadley circulation over the region.

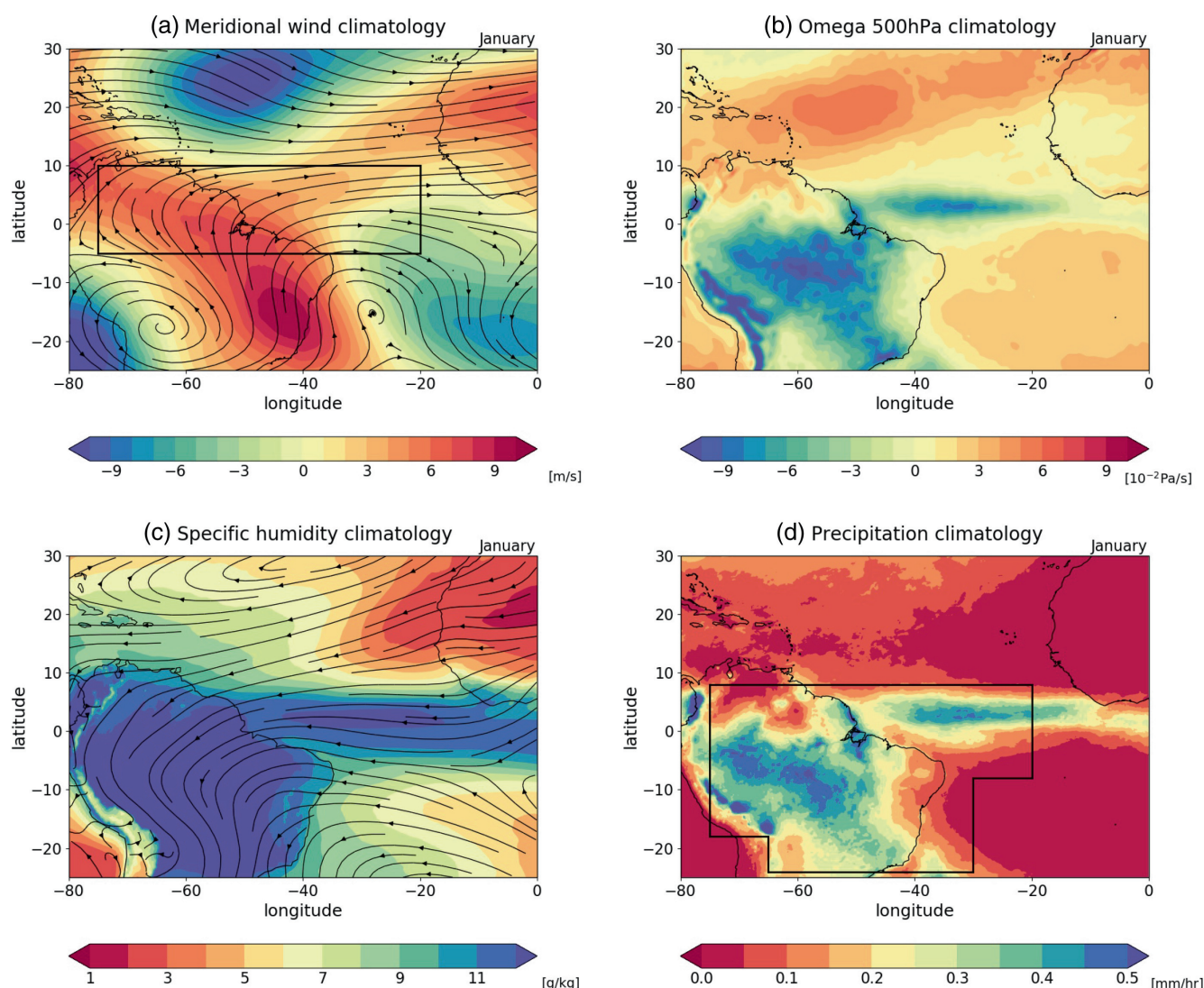


**FIGURE 1** Climatology of (a) 200-hPa meridional wind, (b) pressure velocity at 500 hPa, and (c) specific humidity at 850 hPa for the month of January based on ERA5 data for the years 1991–2020. Streamlines indicate the climatology of horizontal winds at the respective pressure level. (d) Climatology of precipitation based on the GPM observational data set for the years 2001–2021. The boxes in panels (a) and (d) indicate averaging areas for meridional wind and rainfall, respectively, in subsequent Hovmöller plots



The zonal asymmetry is striking, and the important role of the South American continent becomes evident. Over the ocean, the region of ascending motion is narrow and just north of the Equator in January, while over South America the region of deep convection is broad and stretches deep into the Southern Hemisphere, an expression of the South American monsoon system and the South Atlantic Convergence Zone (Liebmann and Mechoso, 2011).

The climatological distribution of specific humidity at 850 hPa indicates that moisture is transported west–southwestward in the Northern Hemisphere and west–northwestward in the Southern Hemisphere to converge over the rainfall-abundant regions (Figure 1c). This is confirmed by the Global Precipitation Measurement (GPM: (Huffman *et al.*, 2019)) precipitation climatology (Figure 1d), which agrees well with the ERA5 midtropospheric vertical velocity field.

Focusing on the aforementioned winter season, Hovmöller diagrams of outgoing longwave radiation (Liebmann and Smith, 1996) and smoothed GPM precipitation agree well on the structure and characteristics of deep convection over the tropical Atlantic (Figure 2, upper row). The month of December stands out to some extent, in that deep convection happens mainly west of 50°W, although there are sporadic strong events also over the ocean. Starting from early January, there are quite distinct periods of prolonged deep convective incidences over the eastern South American continent and the Atlantic.

Organised deep convection occurs at almost all times at some longitudes throughout the season. However, when compositing on periods with strong deep convection in the middle part of the longitude band considered, as indicated by the red vertical lines in Figure 2b, then one can see a strong 200-hPa cross-equatorial meridional flow, mainly over the Atlantic ocean (Figure 2c). In contrast, when compositing on periods during which convection is weak over the central part of the tropical Atlantic (black vertical lines in Figure 2b), the meridional upper-level flow is confined mainly to two centers over land, one in the Northern Hemisphere and one in the Southern Hemisphere, and the cross-equatorial flow is small (Figure 2d). In fact, the upper-level meridional circulation over the Atlantic is even reversed in this case.

The composite analysis suggests that substantial zonal variations occur over time in the locations of deep moist convection, as well as the position and structure of the upper-level meridional circulation, and that both are strongly related. To put this into further context, Figure 3 depicts how the 200-hPa meridional wind and rainfall, averaged over the respective areas as indicated by the boxes in Figure 1a,d, respectively, develop over the 2019/2020 boreal winter season. Although averaging over such spatially extensive regions is a rather crude procedure, it is

evident that there is a close relationship between the two quantities even in an integrated sense, and Figure 3b confirms that winter 2019/2020 is not exceptional in any way. Only a period in mid-December 2019 stands out, when the two variables appear to be anticorrelated rather than correlated. An inspection and comparison of the Hovmöller plots of rainfall (Figure 2b) and meridional wind at 200 hPa (Figure 4a) indicate that a region of enhanced rainfall over the ocean might be responsible for this situation. Since the rainfall area is located north of the Equator (see Figure 1d), it can induce a northerly upper-level flow in some parts of the box over which the meridional wind is averaged. This interpretation is confirmed by computing the correlation between regionally averaged rainfall and 200-hPa meridional wind for each grid box (Figure 4b,c).

When the correlations are computed using the rainfall average only over the oceanic area north of the Equator, then there is a large part of the region that exhibits a negative correlation, implying upper-level northerly flow induced by anomalously enhanced rainfall. As the rainfall is located north of the Equator, this is to be expected and consistent with the previous conclusion that Southern Hemisphere rainfall is driving positive upper-level meridional wind anomalies. A more detailed discussion of the mechanism of how convection can influence circulation over potentially large distances will form the content of the next section.

### 3 | THE TWOFOLD ROLE OF EQUATORIAL WAVES

Investigating the relationship between moist convection and the meridional wind at 200 hPa over the Atlantic region in more detail, the upper left panel in Figure 5 shows GPM precipitation in a Hovmöller diagram overlaid with the  $5 \text{ m}\cdot\text{s}^{-1}$  contour of 200-hPa meridional wind from ERA5. The meridional wind is averaged over the latitudes 5°S–10°N, as indicated by the box in the upper left panel of Figure 1.

In many cases there is a strikingly close correspondence between positive 200-hPa meridional wind and precipitation anomalies. A particularly evident connection between stronger than usual meridional wind and above-average rainfall events can be observed during the periods of December 23–January 10, January 24–29, January 30–February 9, and February 19–February 29. In fact, most of the time there are indications of an intimate link, in terms of both enhancement and abatement, between the intensity of localised moist convective events and longitudinally confined variations in 200-hPa meridional wind.

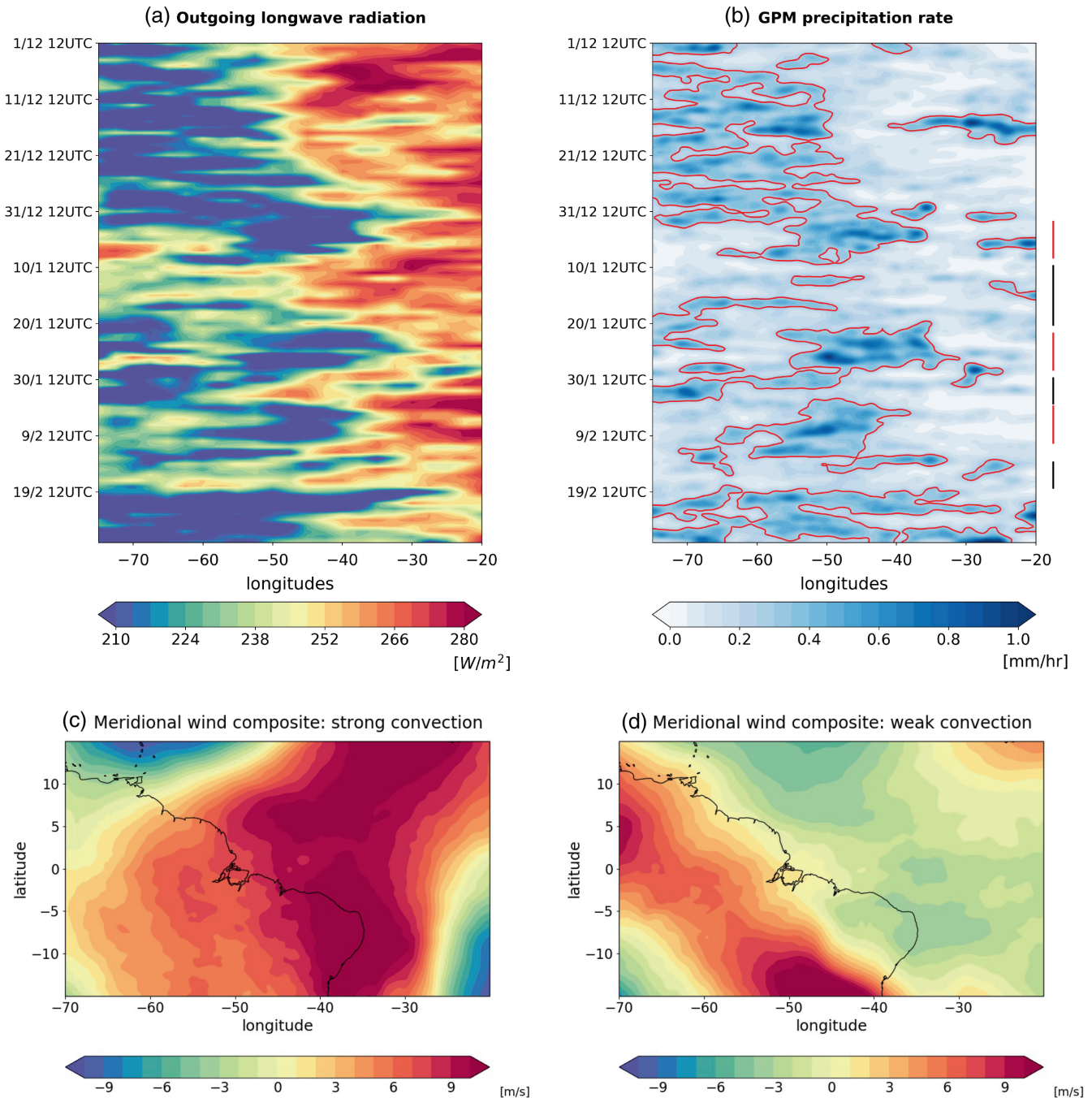


**FIGURE 2** (a) Hovmöller plot of top-of-the-atmosphere outgoing longwave radiation based on daily NOAA data, averaged over latitudes 15°S–5°N. (b) Hovmöller plot of smoothed GPM precipitation rates based on half-hourly data using a Gaussian filter. The region over which the data are averaged in latitude is shown by a box in Figure 1d. The red contour lines indicate the upper tercile of the smoothed data. (c) Composite of 200-hPa meridional wind over periods of strong convection indicated by the vertical red lines in the upper right panel. (d) Composite of 200-hPa meridional wind over periods of weak convection indicated by the vertical black lines in the upper right panel

The precipitation Hovmöller diagram suggests the presence of equatorial waves: both westward- and eastward-moving structures occur. It is therefore natural to examine the ERA5 dynamical fields in more detail and to identify tropical waves independently of

the rainfall data. This is done using the methodology developed in Yang *et al.* (2003). The wave analysis is based on six-hourly ERA5 data of meridional wind, zonal wind, and geopotential height for the tropical belt of 24°S–24°N. A broadband spectral domain with  $k = 2$ –40

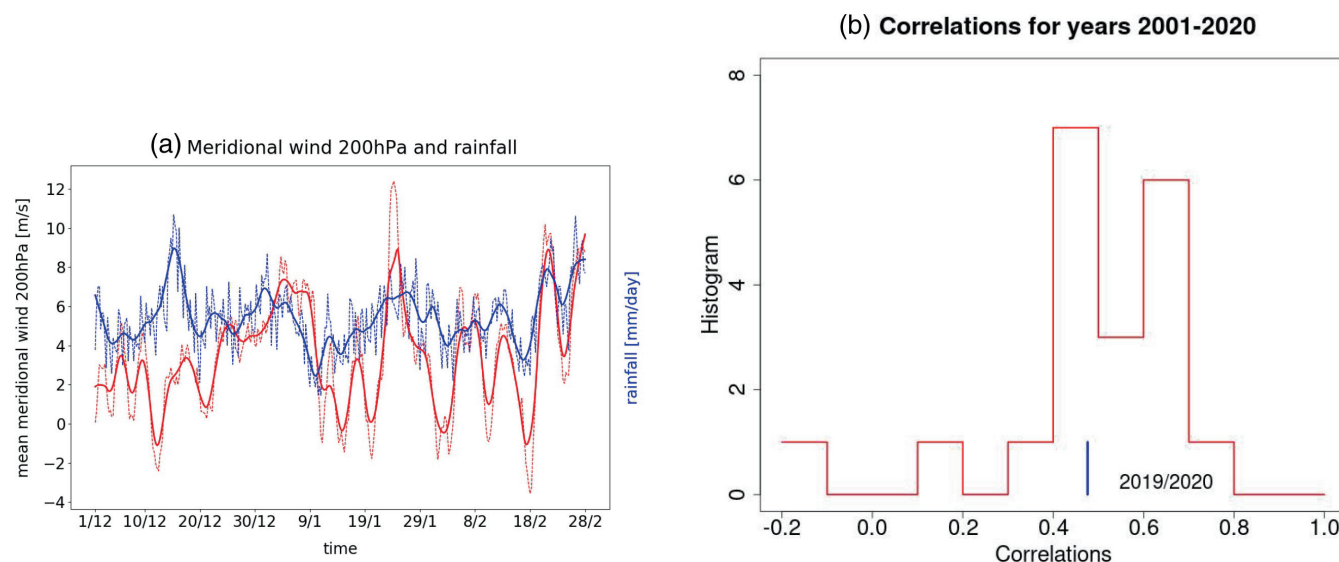


**FIGURE 3** (a) Time series of mean meridional wind at 200 hPa averaged over the box indicated in Figure 1a (red dashed line) and rainfall averaged over the area indicated in Figure 1d (blue dashed line) for the boreal winter 2019/2020. The corresponding solid lines show the same data, but smoothed based on local polynomial regression fitting with span = 0.05. (b) Histogram of correlations between smoothed 200-hPa meridional wind time series and rainfall time series based on the values for the 20 boreal winter seasons 2001–2020. The value for the 2019/2020 season is indicated by a vertical blue line; it is 0.476 and below both the mean and the median of the distribution

is used, and for time-filtered waves a time filter of 1–30 days is applied; this includes all equatorial waves except high-frequency gravity waves (see Yang *et al.* (2021) for more details).

First zonal wind, meridional wind, and geopotential height at 200 hPa are investigated and projected on to different wave patterns, namely westward-moving mixed Rossby–gravity waves (WMRG), eastward-moving mixed Rossby–gravity waves (EMRG), Kelvin waves,  $n = 1$  Rossby waves, and  $n = 2$  Rossby waves. Here the index  $n$  refers to the meridional wave number. The analysis is based on six-hourly data, see Yang *et al.* (2003) for more details.

The most distinct relationship between moist convection and meridional wind components of waves at 200 hPa can be identified in mixed Rossby–gravity waves with no time filtering (Figure 5b, the red lines indicate the  $5 \text{ m s}^{-1}$  contours), in agreement with Hoskins and Yang (2021). Because no time filter is applied, the waves include westward-moving, eastward-moving, and quasistationary mixed Rossby–gravity waves is to be expected due to the eastward mean wind at 200 hPa over the equatorial westerly ducts of the Atlantic and eastern Pacific and the resulting Doppler shift. In some instances, like in the case of the periods January 23–29 and February 5–10, the mixed Rossby–gravity (MRG) wave response to the latent heating from convection occurs

to the east of the main region of latent heat release, as expected based on theoretical grounds (Silva Dias *et al.*, 1984).

The signal in time-filtered eastward-moving mixed Rossby–gravity waves (Figure 5c) and from westward-moving  $n = 1$  Rossby waves (Figure 5d) is generally weaker in magnitude, but there are instances in which latent heating from tropical convection over the region considered seems to play a part in exciting the waves. Kelvin waves do not have a meridional wind component and therefore do not contribute directly to the variability of the meridional flow.

To make the connection between 200-hPa meridional wind variability and the meridional wind component of mixed Rossby–gravity waves more quantitative, Figure 6 shows time series of the two variables for the six boreal winter seasons from 2014/2015 to 2019/2020. The dashed lines display the raw data, and the corresponding solid lines exhibit the smoothed time series. The quantities are averaged over latitudes  $5^{\circ}\text{S}$ – $10^{\circ}\text{N}$  and longitudes  $60^{\circ}$ – $50^{\circ}\text{W}$ , an area chosen in such a way that it is part of the latitude range indicated by the box in Figure 1a, but at the same time reduced in longitudinal extent in order not to average out variability excessively. For each season, the Pearson correlation coefficients were computed; they are indicated in the panels. The results demonstrate that mixed Rossby–gravity waves are the primary mode of variability contributing to large-scale upper-tropospheric



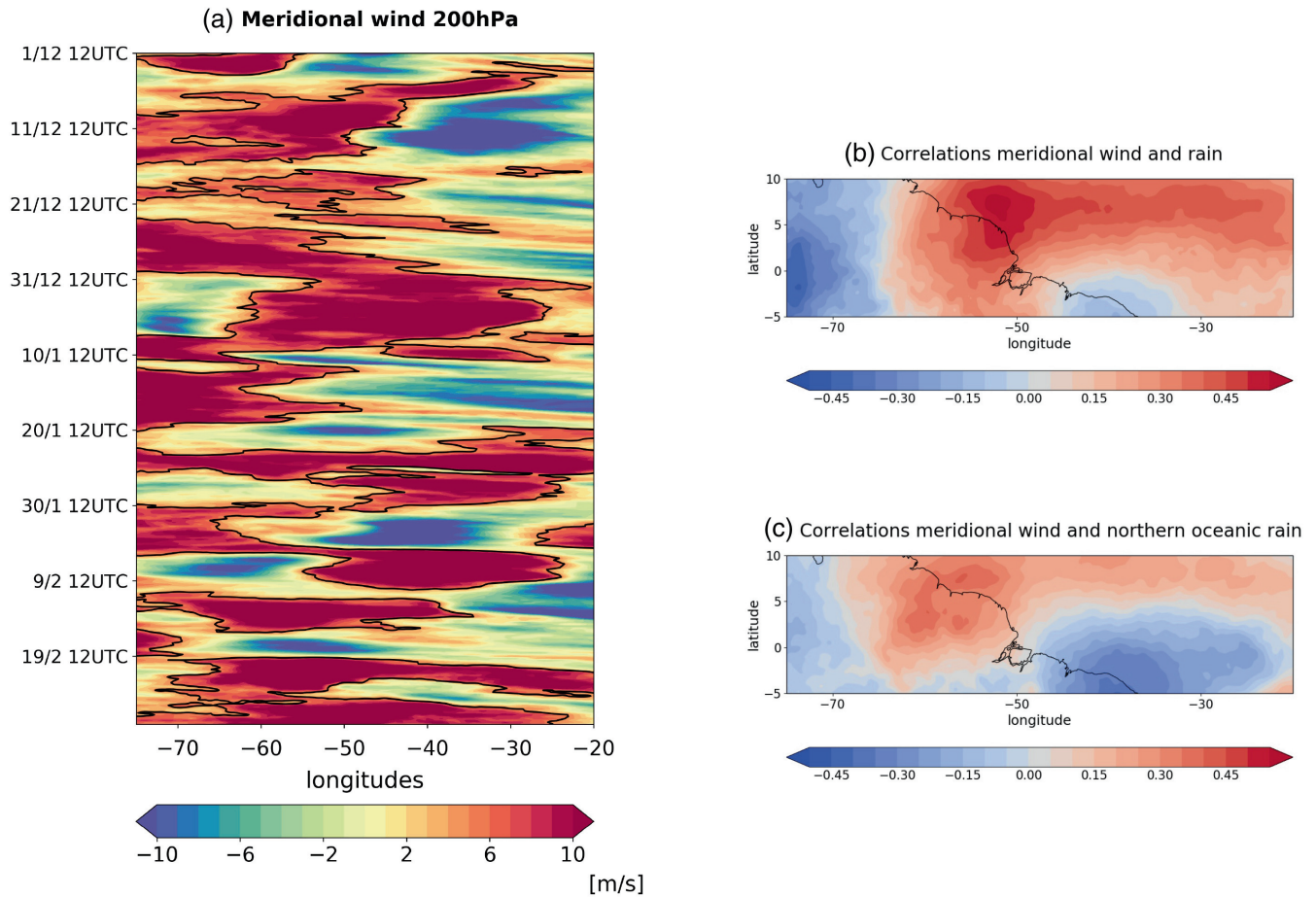


**FIGURE 4** (a) Hovmöller plot of meridional wind at 200 hPa, latitudinally averaged as indicated by the black box in Figure 1a. The  $5 \text{ m} \cdot \text{s}^{-1}$  contour is included. (b) Correlations between mean rainfall averaged over the box indicated in Figure 1d and meridional wind at 200 hPa for each grid box, calculated based on the boreal winter season 2019/2020. (c) Same as in panel (b), but with the rainfall averaged only over the oceanic rainband area north of the Equator (see Figure 1d), namely  $0\text{--}8^\circ\text{N}$  and  $-40$  to  $-20^\circ\text{E}$

meridional wind variations over the subtropical Atlantic during boreal winter.

Latent heat release from moist convection can plausibly drive large-scale circulations (for instance, via equatorial waves as argued in the present study) if the latent heating leads to positive temperature anomalies in the upper troposphere and does not simply adjust the atmosphere back to a neutral state as a response to instabilities created by large-scale processes. That this can indeed be the case is shown in Figure 7. There is notable covariability between rainfall and 300-hPa temperature anomalies over the example region  $60\text{--}50^\circ\text{W}$  and  $15\text{--}5^\circ\text{S}$ . The rainfall here is considered to be a proxy for upper-level latent heat release by moist convection. A rough estimate for the latent heating rate based on the rainfall rate can be obtained by:

$$\text{LH} \approx P \frac{L_c}{\rho \cdot c_p} \approx 2.5 P,$$

where LH is the latent heating rate,  $P$  the precipitation rate,  $\rho$  the density of air,  $c_p$  the specific heat capacity of air at constant pressure, and  $L_c$  the specific latent heat for condensation. Accordingly, the green line in Figure 7a depicts the smoothed rainfall time series scaled by the factor 2.5. The short-term variability of upper-tropospheric temperature anomalies shows similar characteristics over the whole of the season to the latent heating variability estimated based on the rainfall data. The correlation is likely underestimated, because ERA5 latent heating is not expected to be fully consistent with the observed GPM rainfall, and the spatial averaging procedure is inevitably crude. In addition, the bottom two panels show a snapshot of the situation during the Hadley circulation surge event discussed in more detail in Section 4. The spatial pattern of the positive 300-hPa temperature anomaly shows a large-scale extent and correspondence with the regions where organised convection occurs is evident.

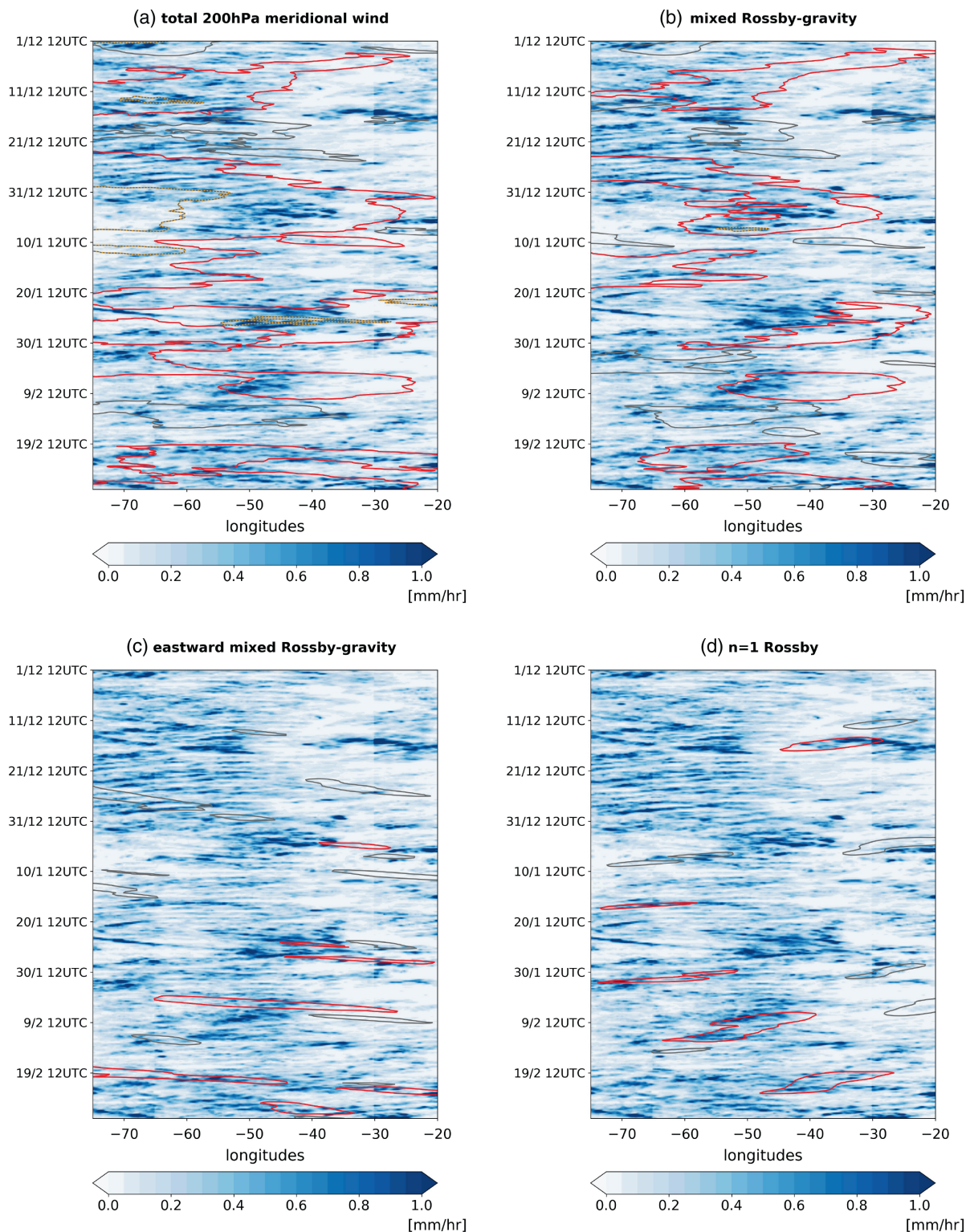


**FIGURE 5** Hovmöller diagrams of (unfiltered) precipitation rates from half-hourly GPM data (blue color shading, the same in all panels) averaged over the latitudes shown by a box in Figure 1d. Overlaid are (a) the  $5 \text{ m} \cdot \text{s}^{-1}$  contours of 200-hPa meridional wind and (b) 200-hPa meridional wind components for different equatorial waves. The meridional wind is averaged over the latitude band  $5^{\circ}\text{S}$ – $10^{\circ}\text{N}$ , except for  $n = 1$  Rossby waves where  $5$ – $15^{\circ}\text{N}$  is used, because that is where the strongest meridional wind anomaly is located in this case (Yang *et al.*, 2003). (b) Mixed Rossby–gravity waves without time filtering. (c) Eastward-moving mixed Rossby–gravity waves. (d)  $n = 1$  Rossby waves. Contours with a longitudinal extent of less than  $8^{\circ}$  have been removed for clarity of presentation. Red contours represent meridional wind periods for which a clear association with enhanced rainfall can be identified; dotted orange contours indicate internal contours inside red contours; gray contours are reserved for meridional wind events during which no clear relationship to positive precipitation anomalies can be detected



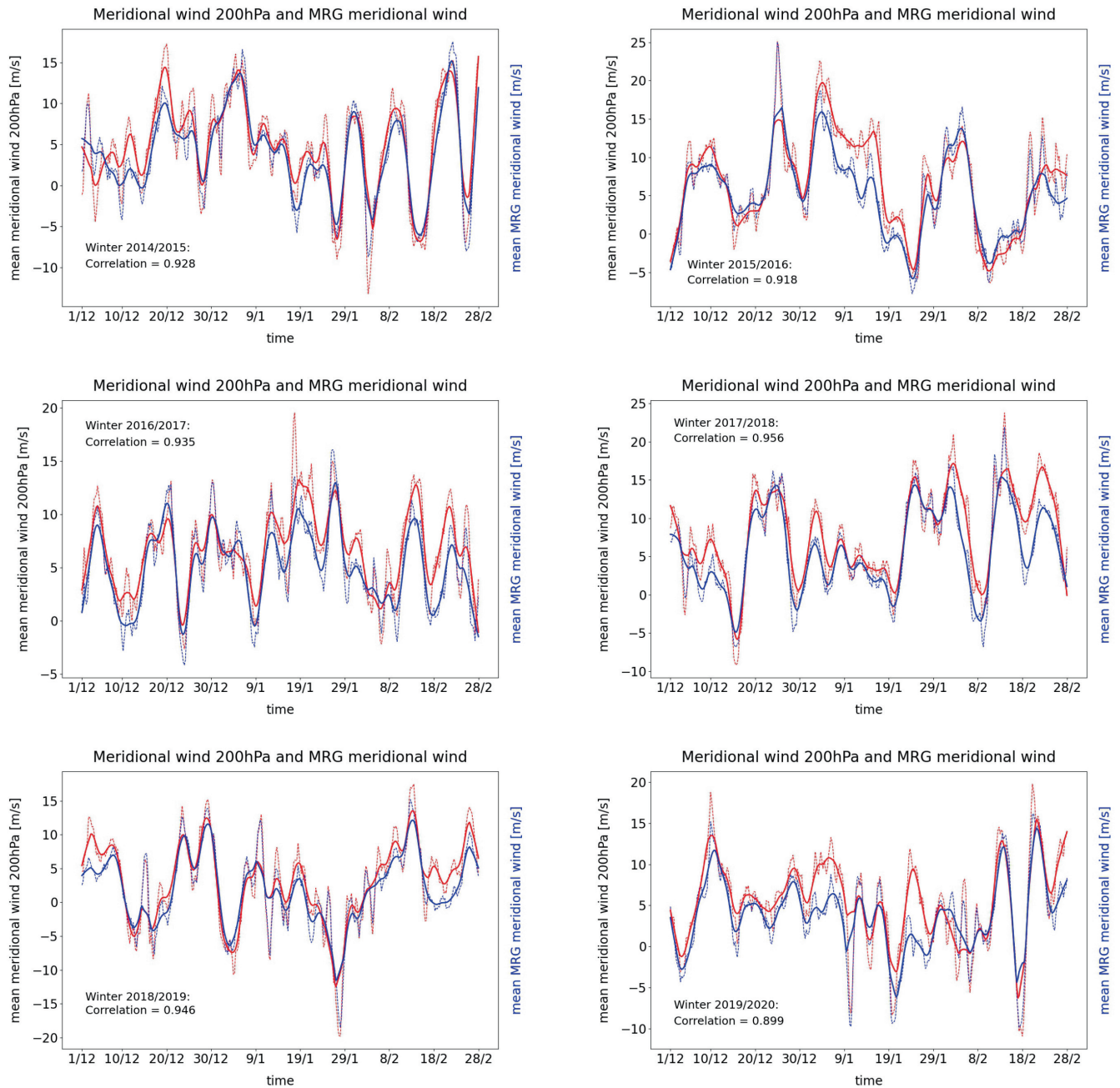


**FIGURE 6** Time series of meridional wind at 200 hPa (dashed red lines) and 200-hPa meridional wind attributed to mixed Rossby–gravity (MRG) waves (dashed blue lines) averaged over latitudes  $5^{\circ}\text{S}$ – $10^{\circ}\text{N}$  and longitudes  $60^{\circ}\text{W}$ – $50^{\circ}\text{W}$  for the six winters from 2014/2015 to 2019/2020. The corresponding solid lines show the same data but smoothed based on local polynomial regression fitting with span = 0.05. The averaging area was chosen in such a way that it is part of the latitude range indicated by the box in Figure 1a, but at the same time reduced in longitudinal extent in order not to average out variability excessively. The Pearson correlations between the two raw time series are also indicated in the panels

Equatorial waves can also impact the Hadley circulation indirectly by spurring moist convection and thus providing the trigger for latent heating and subsequent meridional wind bursts. In this regard, it is appropriate to examine the divergence and convergence signatures of the waves at 850 hPa in the region where moist convection occurs. Eastward-moving features in the rainfall

data are in many cases associated with low-level convergence attributed to Kelvin waves (Figure 8a), but eastward-moving mixed Rossby–gravity waves also play an important role in triggering convection (Figure 8b). Westward-moving precipitating structures are impacted by both westward-propagating mixed Rossby–gravity waves and  $n = 1$  Rossby waves (bottom panels of Figure 8).

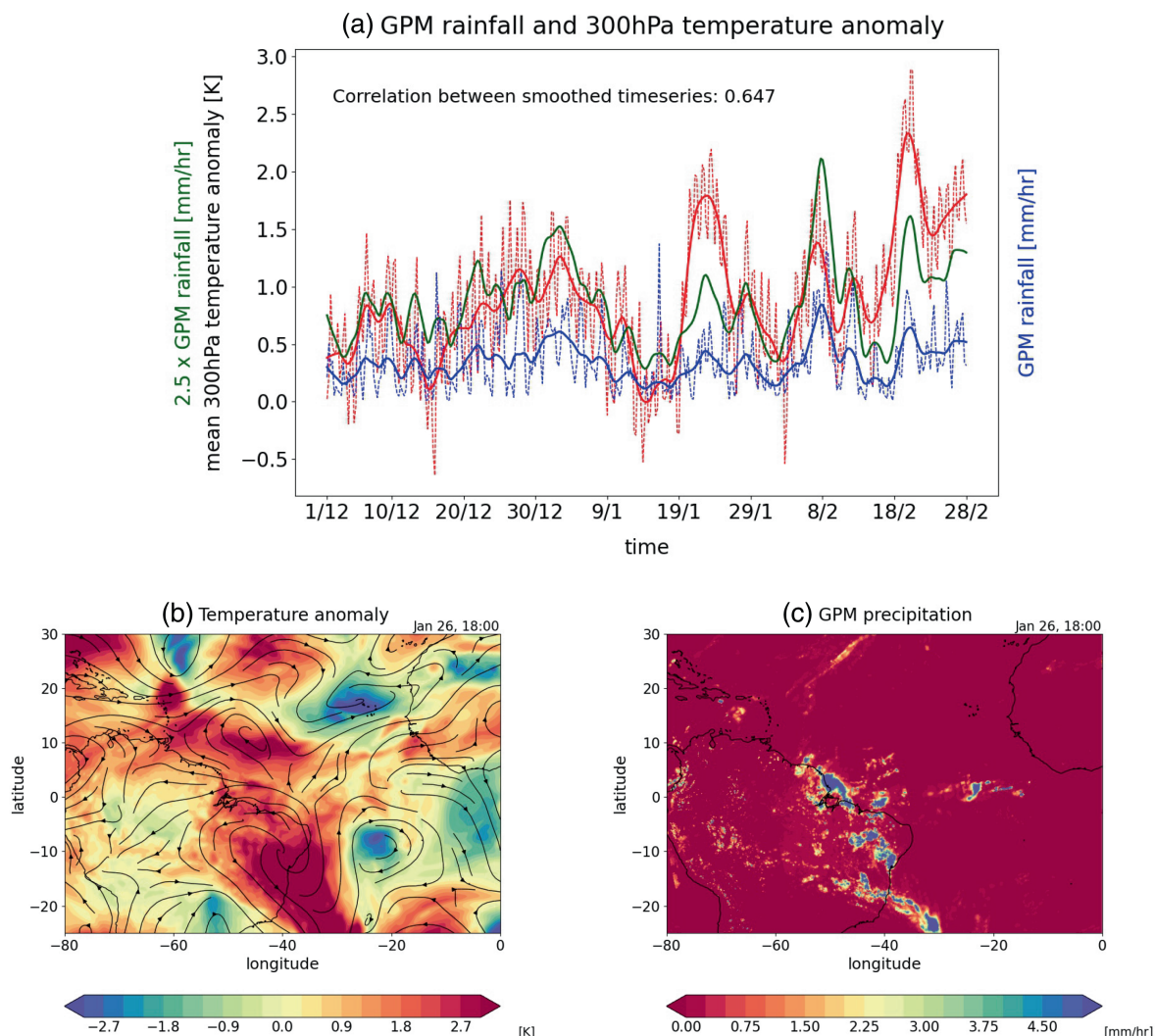


**FIGURE 7** (a) Time series of ERA5 temperature anomalies at 300 hPa (red dashed line) averaged over the area 60–50°W and 15–5°S during winter 2019/2020. The anomalies are calculated with respect to the corresponding monthly climatology over the years 1991–2020. The blue dashed line shows precipitation from GPM averaged over the same area. The corresponding solid lines present the same data but smoothed based on local polynomial regression fitting with span = 0.05. The averaging area was chosen in such a way that it is part of the rainfall box indicated in Figure 1d, but reduced in extent in order not to average out variability excessively. The rainfall is considered a proxy for latent heat release by moist convection. The green line, a rough estimate of the latent heating rate by rainfall formation, is the same as the blue line but scaled by the factor  $2.5 \approx L_c / (\rho \cdot c_p)$ , where  $L_c$  is the specific latent heat of condensation,  $c_p$  the specific heat capacity of air at constant pressure, and  $\rho$  air density. The Pearson correlation between the smoothed time series is indicated. The true correlation is likely underestimated, because ERA5 latent heating is not expected to be fully consistent with GPM rainfall. Also, the spatial averaging is inevitably crude and not well-adjusted to the smaller-scale rainfall structures. (b) ERA5 temperature anomaly at 300 hPa on January 26, 2020, 18:00 UTC. Black streamlines indicate horizontal wind anomalies at 300 hPa. (c) GPM precipitation on the same date and at the same time; the date is part of the Hadley circulation surge period described in more detail in Section 4

In summary, equatorial waves play an important part in mediating the impact of moist convective latent heating on upper-level meridional circulation variability. Without the theory of equatorial wave dynamics, it would be difficult to understand how deep convective clouds, which individually have spatial extents of the order of tens of kilometers, can influence large-scale tropical circulations over distances of thousands of kilometers. The classical Matsuno–Gill model (Matsuno, 1966; Gill, 1980)

provides an explanation that links organised tropical convection with variability in the thermally direct Hadley Cell. Nonequilibrium convection can thus be a source of energy for large-scale motion such as the Hadley Cell via equatorial waves, but also via Madden–Julian-type circulations (Schwendike *et al.*, 2021). By means of modern, high-quality satellite rainfall observation and reanalysis data over the Tropics, the large-scale impact of moist convection in the tropical atmosphere can now be uncovered.



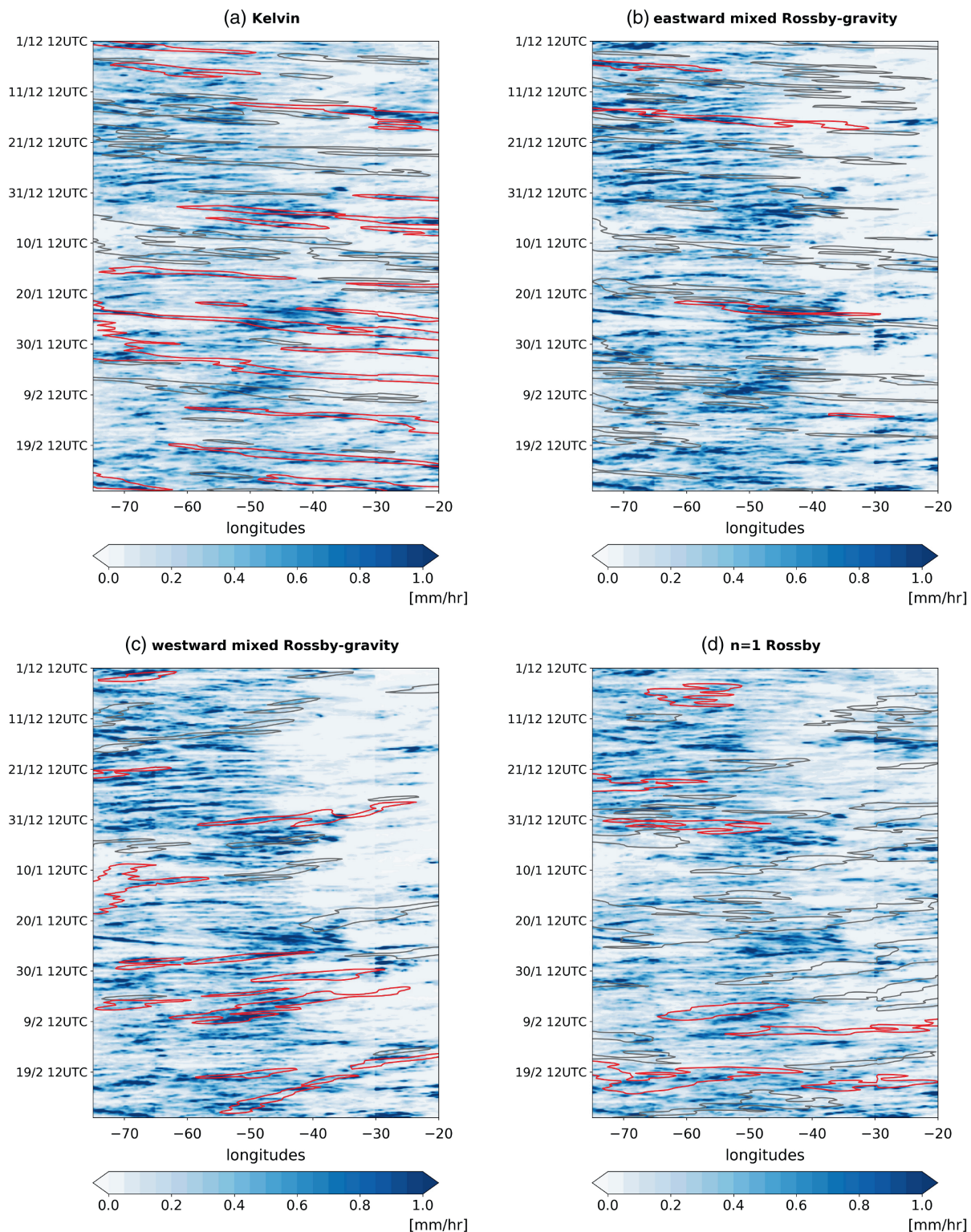


**FIGURE 8** Hovmöller diagrams of precipitation rates from GPM data (blue color shading). Precipitation is averaged over the latitudes shown by a box in the lower right panel of Figure 1, except for WMRG and EMRG waves, for which only the latitudes south of the Equator are used. Overlaid are the  $2.5 \times 10^{-6} \text{ s}^{-1}$  contours of 850-hPa convergence averaged over the same latitudes as the rainfall. Only Southern Hemisphere latitudes are included in the averaging for WMRG and EMRG, because their convergence patterns are antisymmetric relative to the Equator Yang *et al.* (2003). (a) Kelvin waves. (b) Eastward-moving mixed Rossby-gravity waves. (c) Westward-moving mixed Rossby-gravity waves. (d)  $n = 1$  Rossby waves. Contours with a longitudinal extent of less than  $8^\circ$  have been removed for clarity of presentation. Red contours represent convergence periods for which a clear association with enhanced rainfall can be identified; gray contours are reserved for convergence events during which no clear relationship to positive precipitation anomalies can be detected

## 4 | A HADLEY CIRCULATION SURGE EVENT AND THE IMPACT ON TRADE WIND CLOUDINESS

A motivation for the present study, among others, was to understand better the development of larger-scale conditions during the EUREC<sup>4</sup>A observational field campaign and their impact on cloudiness and cloud patterns over the trades. The EUREC<sup>4</sup>A field study took place from January 20, 2020–February 20, 2020, with operations based out of the Caribbean island of Barbados. The observational campaign and the wider project aim to study the life cycle of shallow trade cumulus clouds, associated patterns of convective organization, and the two-way interactions between cloud processes and the larger-scale dynamics (Stevens *et al.*, 2021).

After the weather in the region was influenced by a low-level cold front drifting slowly southward in the northern part of the Atlantic trades during January 17–24 (not shown), cloudiness cleared markedly and the Atlantic subtropical high strengthened significantly over the period from January 25–31, 2020. Some features and how they developed are presented in Figure 9. There was a strong meridional wind anomaly at 200 hPa across the whole of the Tropics, reminiscent of a slow-moving WMRG wave (Figure 9 top panels, see also Figure 5). In the region of enhanced convection, distinct centers of relative vorticity anomalies can be observed (second row in Figure 9) which drive the meridional wind burst. Over the Northern Hemisphere subtropics, upper-level convergence establishes and there is enhanced downward vertical motion (third row in Figure 9, the location of the cross-section is indicated by the black line in the top right panel). The images from the Moderate Resolution Imaging Spectrometer (MODIS) instrument on board the *Terra* satellite demonstrate the effect on cloudiness: over the course of several days, the clouds clear distinctively over the Northern Hemisphere trades.

From the vorticity perspective as put forward by Hoskins *et al.* (2020) and Hoskins and Yang (2021), since the meridional wind anomaly is strong in the Northern Hemisphere during the period, the absolute vorticity is expected to be close to zero. In other words, the positive planetary vorticity in the Northern Hemisphere has to be balanced approximately by upper-level negative relative vorticity. Most of the deep convection occurs in the Southern Hemisphere, where absolute vorticity is negative. Although the relative vorticity anomaly is positive in the location of deep convection over South America, due to this deep convective activity, bursts of negative absolute vorticity air cross the Equator from the Southern Hemisphere into the Northern Hemisphere and approximately

balance the planetary vorticity in the Atlantic Hadley Cell area of the Northern Hemisphere.

This not only demonstrates how tropical convection affects the Hadley circulation on time-scales of days and across thousands of kilometers, but the joint evolution of marked changes in upper-level circulation and low cloud cover over subsidence regions also shows that moist convection and associated Hadley circulation variability can impact cloudiness and cloud patterns over large distances (Myers and Norris, 2013). Similar “divergent surge” events with impacts over 20 degrees of latitude on subtropical high cells were described already in earlier studies such as, for example, Davidson *et al.* (1984). The more detailed understanding of the processes underlying the spatial and temporal variability of the Hadley circulation over the Atlantic region as exemplified in the present case, in particular the roles of organised deep convective systems and associated equatorial waves, complements the time-mean, zonal-mean theory of the Hadley Cell.

## 5 | SUMMARY AND CONCLUSIONS

The present study supports the conceptual perspective on the Hadley circulation introduced and discussed in Hoskins *et al.* (2020) and Hoskins and Yang (2021), and sheds more light on the structure and variability of the Hadley circulation and its close connection to tropical moist convection. The analysis reveals how tropical moist convection drives Atlantic Hadley circulation variability, both temporally and spatially, over large geographic distances on time-scales of days to months mediated by equatorial waves. The evidence suggests that the equatorial waves are, at least partly, instigated by upper-level convective latent heat release in the region.

During the boreal winter season investigated, enhanced deep convective events take place most of the time in some regionally confined areas of the tropical belt considered. During these episodes, upper-level outflow and relative vorticity are distinctly intensified in the locations where convection occurs. This leads to strengthened upper-level flow and thus a reinforced Hadley circulation. The upper-level cross-equatorial flow is strong mainly during periods when there is anomalously intense rainfall in the central part of the tropical Atlantic longitude band. The zonal-mean, time-mean Hadley circulation is composed of such surge events and periods of suppressed convection with weak or even zero cross-equatorial upper-level flow. The enhanced upper-level meridional wind bursts are confined in longitude due to the localized nature of deep convection, and air from the summer hemisphere can reach deep into the opposite winter hemisphere on such occasions.



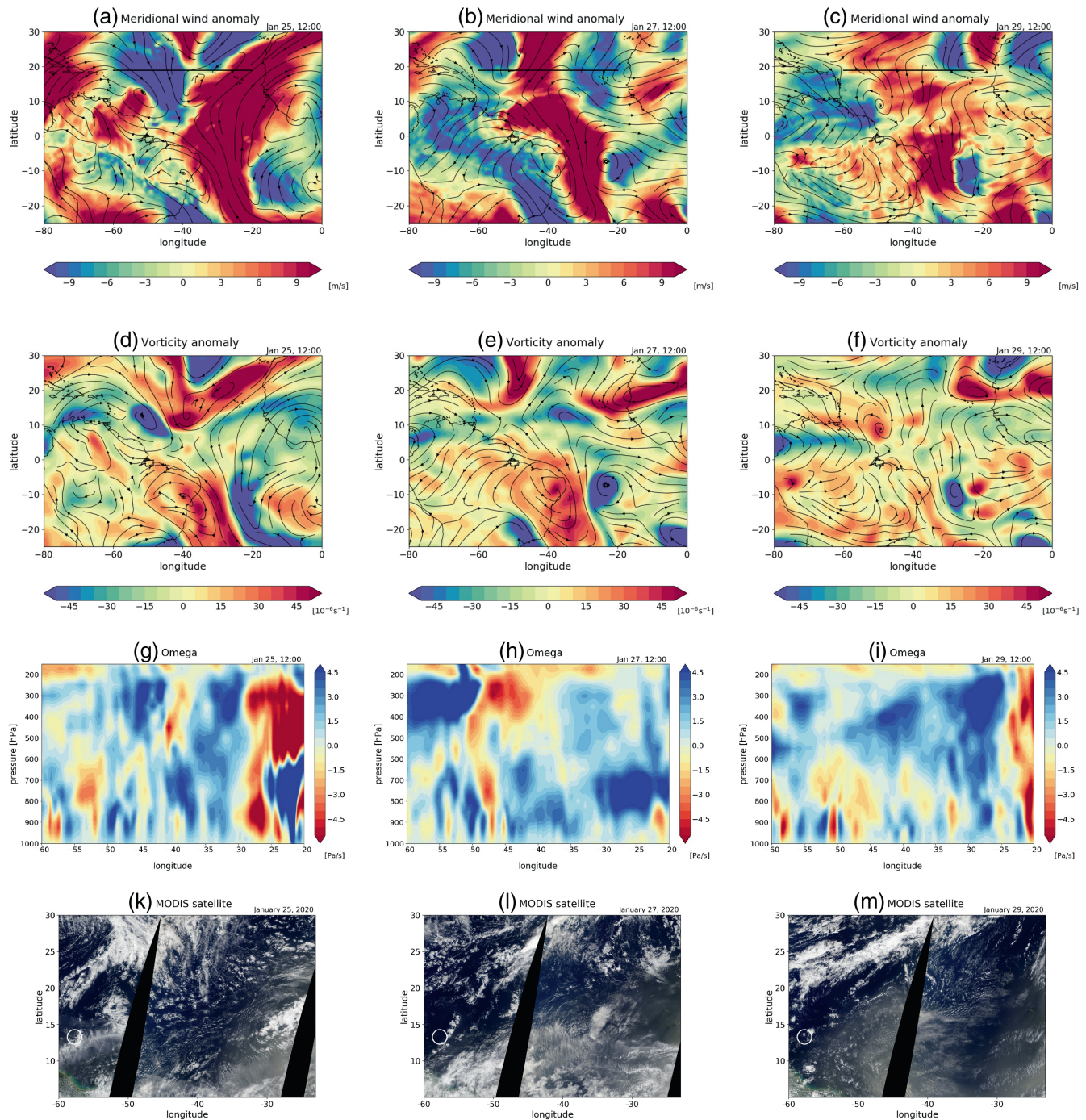


**FIGURE 9** Different diagnostics for three days over the course of the end of January 2020, namely January 25, 27, and 29, 2020. Upper row (a–c): anomaly of 200-hPa meridional wind (and streamlines of horizontal wind anomalies). Second row (d–f): anomaly of relative vorticity at 200 hPa. Third row (g–i): cross-section of pressure velocity along the black line indicated in the top row panels (a–c), averaged over latitudes 18–20°N. Bottom row (k–m): images from the MODIS instrument on board the *Terra* satellite

In many cases, upper-level Hadley circulation variability shows characteristics and structures typically associated with equatorial waves. This is not surprising, given that equatorial waves, beside monsoon circulations, are a main feature of atmospheric dynamics in

the deep Tropics. Equatorial waves can influence Hadley circulation variability in two ways, directly via their meridional wind component and indirectly by exciting moist convection through low-level convergence. The mediation of the influence of tropical moist convection

on the large-scale tropical circulation through equatorial wave dynamics (Matsuno, 1966; Gill, 1980) elucidates the underlying mechanism and explains how moist convection can impact large-scale circulations over distances of thousands of kilometers.

The exact role of moist convection in large-scale tropical, thermally direct overturning circulations like the Hadley and Walker Cells has been debated for many years (Tomassini, 2020). Our results suggest that tropical moist convection and the associated latent heat release, localized in time and space, is an important driver of regional Hadley circulation strength and variability. Although there was anecdotal evidence of this circumstance in the past, the much improved quality of both satellite rainfall observations and reanalysis data in the Tropics available today now allows for a deeper understanding of the intimate coupling between moist convection and circulation in the Tropics over large scales. A more detailed insight into the nature of the interaction between moist convection and winds in low latitudes will help to interpret possible future changes in the tropical circulation better (Held and Soden, 2006; Zaplotnik *et al.*, 2022).

## AUTHOR CONTRIBUTIONS

**Lorenzo Tomassini:** conceptualization; formal analysis; writing – original draft; writing – review and editing.  
**Gui-Ying Yang:** software; writing – original draft; writing – review and editing.


## ACKNOWLEDGEMENTS

The authors thank Brian Hoskins and two anonymous reviewers for insightful comments, which helped to improve the article greatly. G.-Y.Y. was supported by the National Centre for Atmospheric Science ODA national capability programme ACREW (NE/R000034/1), which is supported by NERC and the GCRF.

The ERA5 data Hersbach *et al.* (2020) were downloaded from the Copernicus Climate Change Service (C3S) Climate Data Store (<https://cds.climate.copernicus.eu/cdsapp#!/dataset/reanalysis-era5-pressure-levels>).

The authors acknowledge the use of imagery from the NASA Worldview application (<https://worldview.earthdata.nasa.gov/>), part of the NASA Earth Observing System Data and Information System (EOSDIS). The GPM data Huffman *et al.* (2019) were provided by the NASA/Goddard Space Flight Center, which developed and computed the GPM IMERG dataset as a contribution to the GPM project, and archived at the NASA GES DISC (<https://disc.sci.gsfc.nasa.gov/>). The OLR data Liebmann and Smith (1996) are available at <https://psl.noaa.gov/data/gridded/data.interp/OLR.html>.

## ORCID

Lorenzo Tomassini  <https://orcid.org/0000-0003-3361-7384>

Gui-Ying Yang  <https://orcid.org/0000-0001-7450-3477>

## REFERENCES

- Ayesiga, G., Holloway, C.E., Williams, C.J.R., Yang, G.-Y. and Ferrett, S. (2021) The observed synoptic scale precipitation relationship between Western equatorial Africa and eastern equatorial Africa. *International Journal of Climatology*, 41, 582–601.
- Brown, R.G. and Bretherton, C.S. (1997) A test of the strict quasi-equilibrium theory on long time and space scales. *Journal of the Atmospheric Sciences*, 54, 624–638.
- Cook, K.H. (2003) Role of continents in driving the Hadley cells. *Journal of the Atmospheric Sciences*, 60, 957–976.
- Cook, K.H. (2004) Hadley circulation dynamics: Seasonality and the role of continents. In: Diaz, H.F. and Bradley, R.S. (Eds.) *Advances in Global Change Research The Hadley Circulation: Past, Present, and Future*. Dordrecht: Springer, p. 511.
- Davidson, N.E., McBride, J.L. and McAvaney, B.J. (1984) Divergent circulations during the onset of the 1978–79 Australian monsoon. *Monthly Weather Review*, 112, 1684–1696.
- Emanuel, K.A. (1998) Quasi-equilibrium thinking. In: Randall, D.A. (Ed.) *General Circulation Modelling: Past, Present, and Future*. New York, NY: Academic Press, pp. 225–255.
- Emanuel, K.A., Neelin, J.D. and Bretherton, C.S. (1994) On large-scale circulations in convective atmospheres. *Quarterly Journal of the Royal Meteorological Society*, 120, 1111–1143.
- Ferrett, S., Yang, G.-Y., Woolnough, S., Methven, M.S., Hodges, K. and Holloway, C. (2020) Linking extreme precipitation in South-east Asia to equatorial waves. *Quarterly Journal of the Royal Meteorological Society*, 146, 665–684.
- Fierro, A.O., Simpson, J., LeMone, M.A., Straka, J.M. and Smull, B.F. (2009) On how hot towers fuel the Hadley cell: An observational and modeling study of line-organized convection in the equatorial trough from TOGA COARE. *Journal of the Atmospheric Sciences*, 66, 503–538.
- Gill, A.E. (1980) Some simple solutions for heat-induced tropical circulation. *Quarterly Journal of the Royal Meteorological Society*, 106, 447–462.
- Held, I.M. and Soden, B.J. (2006) Robust responses of the hydrological cycle to global warming. *Journal of Climate*, 19, 5686–5699.
- Hersbach, H., Bell, B., Berrisford, P., et al. (2020) The ERA5 global reanalysis. *Quarterly Journal of the Royal Meteorological Society*, 146, 1999–2049.
- Hoskins, B.J. and Yang, G.-Y. (2021) The detailed dynamics of the Hadley cell Part II: December–February. *Journal of Climate*, 34, 805–823.
- Hoskins, B.J., Yang, G.-Y. and Fonseca, R.M. (2020) The detailed dynamics of the June–August Hadley cell. *Quarterly Journal of the Royal Meteorological Society*, 146, 557–575.
- Huffman, G.J., Stocker, E.F., Bolvin, D.T., Nelkin, E.J. and Tan, J. (2019) *GPM IMERG Final Precipitation L3 Half Hourly 0.1 Degree x 0.1 Degree V06*. Greenbelt, MD: Goddard Earth Sciences Data and Information Services Center (GES DISC).
- Kiladis, G.N., Wheeler, M.C., Haertel, P.T., Straub, K.H. and Roundy, P.E. (2009) Convectively coupled equatorial waves. *Reviews of Geophysics*, 47, RG2003.



- Liebmann, B. and Mechoso, C.R. (2011) The south American monsoon system. In: Chang, C.-P., et al. (Eds.) *The Global Monsoon System: Research and Forecast*. World Scientific Publishing Co., pp. 137–157. <https://www.worldscientific.com/worldscibooks/10.1142/8109#t=aboutBook>
- Liebmann, B. and Smith, C.A. (1996) Description of a complete (interpolated) outgoing longwave radiation dataset. *Bulletin of the American Meteorological Society*, 77, 1275–1277.
- Mapes, B.E. (1997) Equilibrium vs. activation controls on large-scale variations of tropical deep convection. In: Smith, R.L. (Ed.) *The Physics and Parameterization of Moist Convection*. Dordrecht: Kluwer Academic Publishers, pp. 321–358.
- Mapes, B.E. (2000) Convective inhibition, subgrid-scale triggering energy, and stratiform instability in a toy tropical wave model. *Journal of the Atmospheric Sciences*, 57, 1515–1535.
- Matsuno, T. (1966) Quasi-geostrophic motions in the equatorial area. *Journal of the Meteorological Society of Japan*, 44, 25–42.
- Myers, T.A. and Norris, J.R. (2013) Observational evidence that enhanced subsidence reduces subtropical marine boundary layer cloudiness. *Journal of Climate*, 26, 7507–7524.
- Neelin, J.D. and Zeng, N. (2000) A quasi-equilibrium tropical circulation model - formulation. *Journal of the Atmospheric Sciences*, 57, 1741–1766.
- Pan, D.M. and Randall, D.A. (1998) A cumulus parameterization with a prognostic closure. *Quarterly Journal of the Royal Meteorological Society*, 124, 949–981.
- Riehl, H. and Malkus, J.S. (1958) On the heat balance in the equatorial trough zone. *Geophysica*, 6, 503–538.
- Schwendike, J., Berry, G.J., Fodor, K. and Reeder, M.J. (2021) On the relationship between the madden-Julian oscillation and the Hadley and Walker circulations. *Journal of Geophysical Research: Atmospheres*, 126, e2019JD032117.
- Schwendike, J., Berry, G.J., Reeder, M.J., Jakob, C., Govekar, P. and Wardle, R. (2015) Trends in the local Hadley and local Walker circulations. *Journal of Geophysical Research: Atmospheres*, 120, 7599–7618.
- Silva Dias, P.L., Schubert, W.H. and DeMaria, M. (1984) Large-scale response of the tropical atmosphere to transient convection. *Journal of the Atmospheric Sciences*, 40, 2689–2707.
- Stevens, B., Bony, S., Farrell, D., Ament, F., Blyth, A., Fairall, C., Karstensen, J., Quinn, P.K., Speich, S., Acquistapace, C., Aemisegger, F., Albright, A.L., Bellenger, H., Bodenschatz, E., Caesar, K.-A., Chewitt-Lucas, R., de Boer, G., Delanoë, J., Denby, L., Ewald, F., Fildier, B., Forde, M., George, G., Gross, S., Hagen, M., Hausold, A., Heywood, K.J., Hirsch, L., Jacob, M., Jansen, F., Kinne, S., Klocke, D., Kölling, T., Konow, H., Lothon, M., Mohr, W., Naumann, A.K., Nuijens, L., Olivier, L., Pincus, R., Pöhlker, M., Reverdin, G., Roberts, G., Schnitt, S., Schulz, H., Siebesma, A.P., Stephan, C.C., Sullivan, P., Touzé-Peiffer, L., Vial, J., Vogel, R., Zuidema, P., Alexander, N., Alves, L., Arixi, S., Asmath, H., Bagheri, G., Baier, K., Bailey, A., Baranowski, D., Baron, A., Barrau, S., Barrett, P.A., Batier, F., Behrendt, A., Bendinger, A., Beucher, F., Bigorre, S., Blades, E., Blossey, P., Bock, O., Böing, S., Bosser, P., Bourras, D., Bouruet-Aubertot, P., Bower, K., Branellec, P., Branger, H., Brennek, M., Brewer, A., Brilouet, P.-E., Brüggemann, B., Buehler, S.A., Burke, E., Burton, R., Calmer, R., Canonici, J.-C., Carton, X., Gregory Cato, J.A.C., Jr., Chazette, P., Chen, Y., Chilinski, M.T., Choularton, T., Chuang, P., Clarke, S., Coe, H., Cornet, C., Coutris, P., Couvreur, F., Crewell, S., Cronin, T., Cui, Z., Cuypers, Y., Daley, A., Damerell, G.M., Dauhut, T., Deneke, H., Desbios, J.-P., Dörner, S., Donner, S., Douet, V., Drushka, K., Dütsch, M., Ehrlich, A., Emanuel, K., Emmanouilidis, A., Etienne, J.-C., Etienne-Leblanc, S., Faure, G., Feingold, G., Ferrero, L., Fix, A., Flamant, C., Flatau, P.J., Foltz, G.R., Forster, L., Furtuna, I., Gadian, A., Galewsky, J., Gallagher, M., Gallimore, P., Gaston, C., Gentemann, C., Geyskens, N., Giez, A., Gollop, J., Gouirand, I., Gourbeyre, C., de Graaf, D., de Groot, G.E., Grosz, R., Güttler, J., Gutleben, M., Hall, K., Harris, G., Helfer, K.C., Henze, D., Herbert, C., Holanda, B., Ibanez-Landeta, A., Intrieri, J., Iyer, S., Julien, F., Kalesse, H., Kazil, J., Kellman, A., Kidane, A.T., Kirchner, U., Klingebiel, M., Körner, M., Kremper, L.A., Kretschmar, J., Krüger, O., Kumala, W., Kurz, A., L'Hégaret, P., Labaste, M., Lachlan-Cope, T., Laing, A., Landschützer, P., Lang, T., Lange, D., Lange, I., Laplace, C., Lavik, G., Laxenaire, R., Le Bihan, C., Leandro, M., Lefevre, N., Lena, M., Lenschow, D., Li, Q., Lloyd, G., Los, S., Losi, N., Lovell, O., Luneau, C., Makuch, P., Malinowski, S., Manta, G., Marinou, E., Marsden, N., Masson, S., Maury, N., Mayer, B., Mayers-Als, M., Mazel, C., McGeary, W., McWilliams, J.C., Mech, M., Mehlmann, M., Meroni, A.N., Mieslinger, T., Minikin, A., Minnett, P., Möller, G., Avalos, Y.M., Muller, C., Musat, I., Napoli, A., Neuberger, A., Noisel, C., Noone, D., Nordsiek, F., Nowak, J.L., Oswald, L., Parker, D.J., Peck, C., Person, R., Philippi, M., Plueddemann, A., Pöhlker, C., Pörtge, V., Pöschl, U., Pologne, L., Posyniak, M., Prange, M., Meléndez, E.Q., Radtke, J., Ramage, K., Reimann, J., Renault, L., Reus, K., Reyes, A., Ribbe, J., Ringel, M., Ritschel, M., Rocha, C.B., Rochetin, N., Röttenbacher, J., Rollo, C., Royer, H., Sadoulet, P., Saffin, L., Sandiford, S., Sandu, I., Schäfer, M., Schemann, V., Schirmacher, I., Schlenczek, O., Schmidt, J., Schröder, M., Schwarzenboeck, A., Sealy, A., Senff, C.J., Serikov, I., Shohan, S., Siddle, E., Smirnov, A., Späth, F., Spooner, B., Stolla, M.K., Szkółka, W., de Szoeko, S.P., Tarot, S., Tetoni, E., Thompson, E., Thomson, J., Tomassini, L., Totems, J., Ubele, A.A., Villiger, L., von Arx, J., Wagner, T., Walther, A., Webber, B., Wendisch, M., Whitehall, S., Wiltshire, A., Wing, A.A., Wirth, M., Wiskandt, J., Wolf, K., Worbes, L., Wright, E., Wulfmeyer, V., Young, S., Zhang, C., Zhang, D., Ziemann, F., Zinner, T. and Zöger, M. (2021) EUREC<sup>4</sup>a. *Earth System Science Data*, 13, 4067–4119.
- Stevens, B., Randall, D.A., Lin, X. and Montgomery, M.T. (1997) Comments on 'On large-scale circulations in convecting atmospheres' by Kerry a. Emanuel, J. David Neelin, and Christopher S Bretherton. *Quarterly Journal of the Royal Meteorological Society*, 123, 1771–1778.
- Tomassini, L. (2020) The interaction between moist convection and the atmospheric circulation in the tropics. *Bulletin of the American Meteorological Society*, 101, 1378–1396.
- Yang, G.-Y., Ferrett, S., Woolnough, S., Methven, J. and Holloway, C. (2021) Real-time identification of equatorial waves and evaluation of waves in global in global forecasts. *Weather and Forecasting*, 36, 171–193.
- Yang, G.-Y., Hoskins, B. and Slingo, J. (2003) Convectively coupled equatorial waves: A new methodology for identifying wave structures in observational data. *Journal of the Atmospheric Sciences*, 60, 1637–1654.
- Yang, G.-Y., Hoskins, B. and Slingo, J. (2007a) Convectively coupled equatorial waves. Part I: horizontal structure. *Journal of the Atmospheric Sciences*, 64, 3406–3423.
- Yang, G.-Y., Hoskins, B. and Slingo, J. (2007b) Convectively coupled equatorial waves. Part II: Propagation characteristics. *Journal of the Atmospheric Sciences*, 64, 3424–3437.

- Yang, G.-Y., Hoskins, B. and Slingo, J. (2007c) Convectively coupled equatorial waves. Part III: Synthesis structures and their forcing and evolution. *Journal of the Atmospheric Sciences*, 64, 3438–3451.
- Yano, J.-I. and Plant, R. (2012) Interactions between shallow and deep convection under a finite departure from convective quasi equilibrium. *Journal of the Atmospheric Sciences*, 69, 3463–3470.
- Zaplotnik, Z., Pikovnik, M. and Boljka, L. (2022) Recent Hadley circulation strengthening: A trend or multidecadal variability? *Journal of Climate*, 35, 4157–4176.

**How to cite this article:** Tomassini, L. & Yang, G.-Y. (2022) Tropical moist convection as an important driver of Atlantic Hadley circulation variability. *Quarterly Journal of the Royal Meteorological Society*, 148(748), 3287–3302. Available from: <https://doi.org/10.1002/qj.4359>